Quantum-dot-assisted characterization of microtubule rotations during cargo transport

BERT NITZSCHE, FELIX RUHNOW AND STEFAN DIEZ*

Max Planck Institute of Molecular Cell Biology and Genetics, 01307 Dresden, Germany
***e-mail: diez@mpi-cbg.de**

Published online: 10 August 2008; doi:10.1038/nnano.2008.216

Owing to their wide spectrum of *in vivo* functions, motor proteins, such as kinesin-1, show great potential for application as nanomachines in engineered environments. When attached to a substrate surface, these motors are envisioned to shuttle cargo that is bound to reconstituted microtubules—one component of the cell cytoskeleton—from one location to another[1,2]. One potentially serious problem for such applications is, however, the rotation of the microtubules around their longitudinal axis[3,4]. Here we explore this issue by labelling the gliding microtubules with quantum dots to simultaneously follow their sinusoidal side-to-side and up-and-down motion in three dimensions with nanometre accuracy. Microtubule rotation, which originates from the kinesin moving along the individual protofilaments of the microtubule, was not impeded by the quantum dots. However, pick-up of large cargo inhibited the rotation but did not affect the velocity of microtubule gliding. Our data show that kinesin-driven microtubules make flexible, responsive and effective molecular shuttles for nanotransport applications.

The linear motion of motor proteins along microtubules has been studied in detail using stepping assays with motor-coated microbeads[5,6], motor-attached quantum dots (QDs)[7,8] or single fluorescently labelled motors[9,10]. However, microtubules are three-dimensional (3D) nanostructures on the surface of which motor proteins can move on nonlinear trajectories. As a consequence, regular off-axis stepping of motors will lead to microtubule rotation in gliding assays, where the microtubules are propelled by substrate-attached motor proteins. Such gliding assays are most promising for nanotransport applications in synthetic environments[1,2], where it is envisioned that the surface of the gliding filaments will be used for cargo pick-up[11] and delivery[12]. However, filament rotation will then force large cargo to interact with the substrate surface. Because dimeric kinesin-1 motors have been shown to follow individual protofilaments of supertwisted microtubules in a robust manner (note that the micrometre-long kink structures in refs 3 and 4 did not cause the cessation of rotational movement), one might expect the cargo either to be stripped off or the forward motion of the gliding microtubules to be impaired due to the sideways load on the individual motors[13].

To investigate microtubule rotation with high accuracy, we sparsely labelled reconstituted microtubules with QDs[14–16] and used fluorescence microscopy with arc-lamp illumination to image their longitudinal and rotational movement over reflective silicon surfaces coated with dimeric kinesin-1 motor proteins (Fig. 1). We determined the two-dimensional (2D) *xy*-positions of the QDs with subpixel accuracy by nanometre tracking[17] and combined these data with simultaneous height measurements based on fluorescence-interference contrast (FLIC) microscopy[18] (see Supplementary Information for discussion of the tracking accuracy and temporal resolution of the method). FLIC, which is based on interference effects between the direct excitation and emission light with reflected light from the surface, leads to a periodic modulation of the detected emission intensity as a function of height above the surface. Minimum intensity is observed directly on the surface, and the first maximum is located ~100–150 nm above the surface. Thus, QDs (diameter of ~20 nm) attached to rotating microtubules (diameter of 25 nm) gliding at an average height of about 30 nm (ref. 19) were expected to periodically change their emission intensity as they are moved up and down above the surface.

When filament rotation had been studied previously, optical detection relied on filament supercoiling[20,21] or periodic sideways deflections of distinctive microtubule structures (artificial kinks or axoneme doublets with lengths in the micrometre range)[3,4,22,23]. As a consequence, these experiments had a limited accuracy with respect to quantification of the rotational periodicities and were based on the deliberate construction of impaired gliding assays or defective filaments. In contrast, in the present experiments, given the contour length of ~60 nm for the kinesin-1 constructs, it was expected that the QDs used as optical reporters would have no impact on the rotations.

From a maximum projection of the QD signals over time (Fig. 2a) a periodic variation in intensity along the path of the microtubule is directly visible. Quantitative fluorescence data as a function of distance travelled by the microtubules were obtained by tracking the intensity values and the *xy*-positions of the QDs for each frame of the recorded time series (Fig. 2b). For statistical treatment we investigated the transport of 146 QDs (on 98 microtubules). We rejected 41 of the QD traces because the traces were shorter than 15 μm (about twice the length of the expected supertwist for a microtubule with 14 protofilaments), the overall QD signal was too low, or a perturbing event such as microtubule crossing occurred. We then categorized the remaining events into the following classes: 94% rotating (showing at least two clear maxima or minima), 5% non-rotating and 1% unclear (that is, non-classifiable) events. Plotting

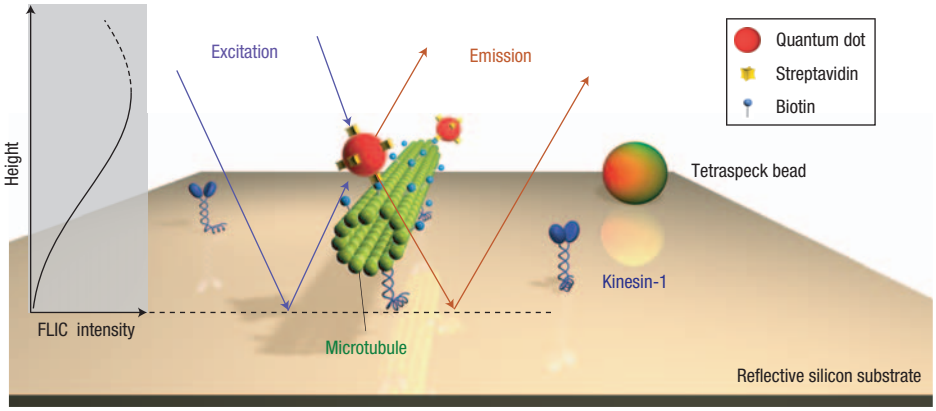

Figure 1 Principle of QD-assisted 3D imaging of microtubule rotation. QDs are attached to motor-propelled, fluorescently labelled microtubules by means of biotin–streptavidin linkage. Imaging is performed by dual-colour fluorescence microscopy. Owing to fluorescence-interference contrast, the recorded fluorescence intensities increase as a function of distance above the substrate surface. To avoid low fluoresence intensity of objects near the reflective silicon substrate, the surface is primed with a 30-nm transparent silicon oxide layer (not shown). Multi-fluorescent tetraspeck beads are used for spatial alignment when superimposing the images from the different colour channels.

the periodicities of the rotating events into a histogram (Fig. 2c) revealed a main peak with an average periodicity of 7.86 ± 1.37 μm (mean ± s.d., $n = 99$). This value matches our expectation because it is known that (1) according to electron microscopy studies ~95% of the microtubules grown in the presence of guanylyl-(α,β)-methylene-diphosphonate (GMP-CPP) are composed of 14 protofilaments[24], leading to a characteristic left-handed supertwist with a pitch between 7.75 ± 0.33 μm (J. Howard, personal communication) and 8.95 ± 1.36 μm (ref. 24), and (2) that kinesin-1 follows the protofilament axis of microtubules[3,5]. Three other microtubule preparation protocols, leading to increased percentages of microtubules composed of 12 and 13 protofilaments, yielded periodicities in accordance with earlier electron microscopy studies (see Supplementary Information).

When tracking multiple QDs on a single GMP-CPP microtubule we found a periodicity of 7.90 ± 0.65 μm (mean ± s.d., $n = 4$ measured periods) for the first QD and a period of 7.84 ± 0.32 μm (mean ± s.d., $n = 3$) for the second QD. This agreement indicates the robustness of our method and points towards the absence of detrimental effects related to the build-up of internal torsion in the microtubule during transport.

We then questioned whether modifications on the microtubule lattice can alter the paths of motor proteins. For example, it has been shown that the negatively charged C-terminus of tubulin, also known as 'E-hook', interacts with kinesin-1, conferring increased speed and processivity to the motor protein[25]. We performed experiments to find out whether the E-hook is necesssary for kinesin-1 to track the protofilament axis of a microtubule. Analysis of gliding GMP-CPP microtubules whose E-hooks had been cleaved off by subtilisin (see Supplementary Information) revealed an average periodicity of 8.37 ± 0.17 μm (mean ± s.e.m., total number of detected periods = 55, from 12 microtubules). In control measurements, undigested GMP-CPP microtubules displayed a periodicity of 7.98 ± 0.16 μm (mean ± s.e.m., total number of detected periods = 71, from 15 microtubules). Performing a *t*-test on these data we obtained a *t*-value of 1.65. Thus, there is no evidence (at 95% confidence level) that kinesin-1 requires the interaction with the tubulin E-hook in order to track the microtubule protofilament axis.

Although FLIC microscopy on its own is a convenient tool to determine the periodicities of microtubule rotations, it does not allow deduction of the handedness of rotation. To obtain this piece of information we performed simultaneous dual-colour FLIC imaging (Fig. 3a) and tracked the *xy*-positions of the microtubules (emitting in the green) in addition to the QD positions (emitting in the red). We calculated the sideways deviation of the QDs from the microtubules for each frame of the recorded time series. The resulting sinusoidal curves exhibited the same periodicities as the FLIC intensity curves (Fig. 3b,c). Combining the information of both curves, the QD positions with respect to the moving microtubule could be reconstructed in 3D and the orientation of microtubule rotation could be directly deduced (see also Supplementary Information).

Using our method, we directly investigated what happens to the rotational movement of gliding microtubules during the pick-up of large cargo (Fig. 4). We used QD-assisted FLIC measurements to detect the rotations of unladen GMP-CPP microtubules and observed *in situ* how the rotational behaviour changed when the microtubules picked up 2.8-μm beads from the solution, the substrate surface or other microtubules (Fig. 4a–c). Once loaded onto the microtubules, most of the beads were transported over distances longer than the observation area. In these cases the rotations stopped upon cargo pick-up with minimal impact on the forward speed of the gliding microtubules (speed before pick-up 676 ± 14 nm s^{-1}, slow-down of the individual microtubules after pick-up 4.1 ± 2.0%, mean ± s.d., $n = 13$ microtubules). The inverse behaviour was observed when a bead-carrying microtubule dropped off its cargo and resumed its rotational motion (Fig. 4d–f).

In an earlier study[4] using monomeric, non-processive kinesin-1 it was shown that a long kinked structure in the microtubule could also block the torsional motion without an effect on the forward speed. However, this behaviour could be well explained by the possibility that a non-processive motor can always freely choose the nearest protofilament for the next step. In contrast, our study is the first evidence of such behaviour for dimeric, processive kinesin-1, which is assumed to follow the axis of an individual protofilament during its whole run. The sideways load, which accumulates on the

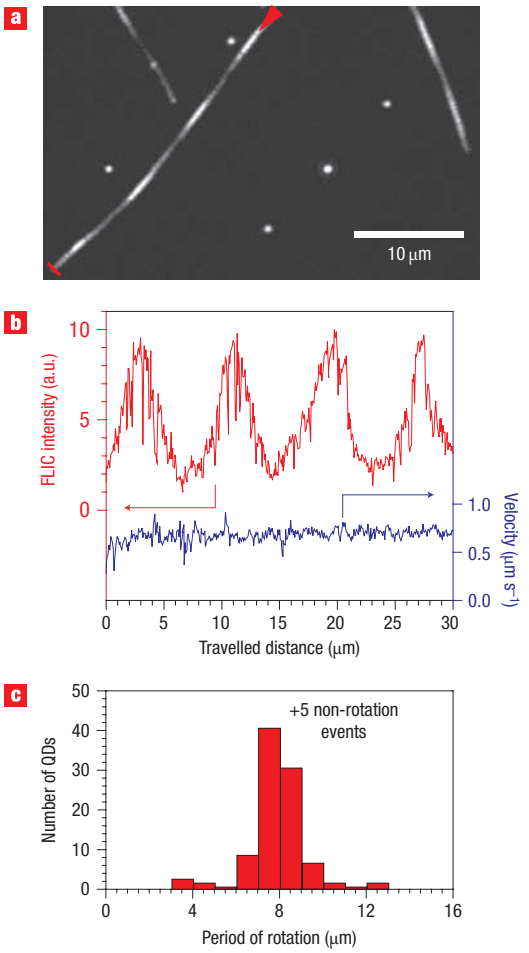

Figure 2 FLIC microscopy of QDs attached to microtubules driven by kinesin-1. a, Characteristic maximum projection of QD signals over time (see Supplementary Information, Movie 1). **b**, Typical intensity (red) and velocity (blue) traces versus distance travelled for a QD attached to a gliding microtubule. Data correspond to the marked maximum projection in **a**. **c**, Histogram of measured rotational periodicities on kinesin-1-coated surfaces (periodicity = 7.86 ± 1.37 μm, mean ± s.d., $n = 99$). Microtubules were self-assembled in the presence of GMP-CPP.

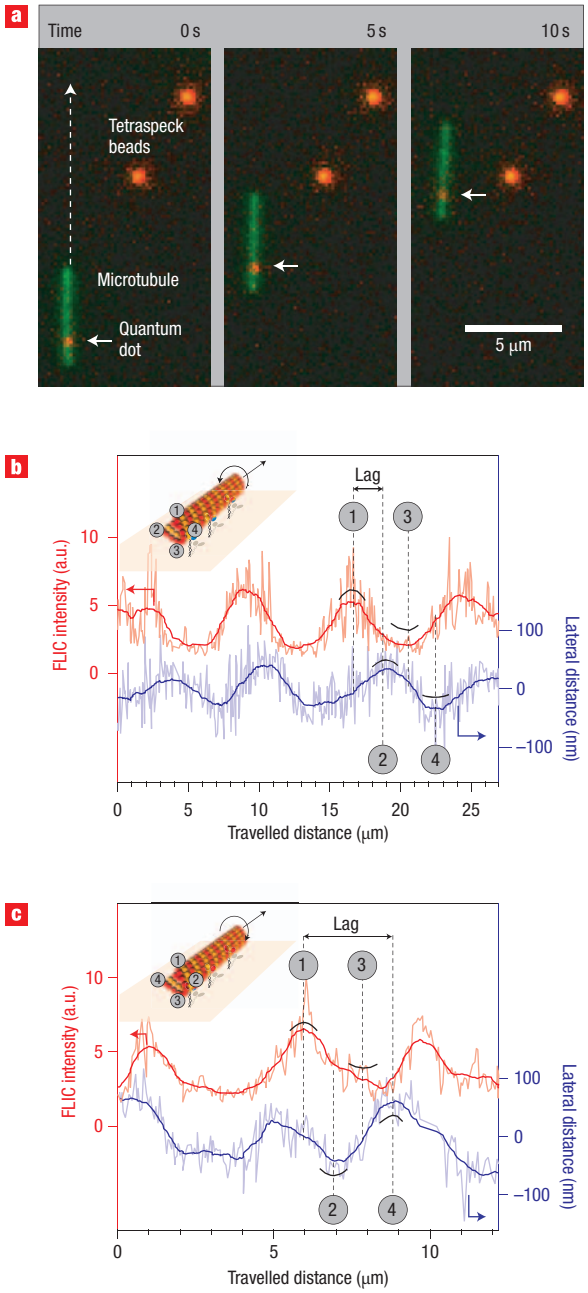

Figure 3 Determining the direction of rotation using dual-colour FLIC imaging. a, Time series of motile microtubule (green) with attached QD (red) (image acquisition rate: 10 frames s^{-1}). **b**, *xy*-deviation of the QD from the microtubule (lateral distance) and FLIC intensity versus distance travelled for a 14-protofilament GMP-CPP microtubule (typical rotation period ~8 μm). Inset: counterclockwise rotation (looking in the direction of motion) derived from the temporal sequence of the 3D positions relative to the microtubule. **c**, Clockwise rotation of a 12-protofilament microtubule (typical rotation period ~4 μm) assembled in the presence of GTP and taxol[24,28,29].

individual motors during these runs, might be expected to impair the microtubule forward movement[13]. However, the lack of such impairment hints towards the release of the sideways strain caused by kinesin-1 motors switching protofilaments either during their runs or during short periods of detachment from the microtubule. The latter possibility might be supported by the limited run length of kinesin-1 in comparison to the periodicity of the supertwist as well as by the additional decrease of the run length caused by sideways forces on the motors[13].

We have described a novel method to characterize the rotational movement of cytoskeletal filaments gliding over motor-coated substrate surfaces. Although the labelling of the microtubules with QDs did not impede the rotational movement, the pick-up of larger cargo did. However, the fact that the velocity of microtubule gliding was not affected shows that kinesin-driven microtubules make flexible, responsive and effective molecular shuttles for nanotransport applications. Beyond the application to cytoskeletal motor proteins we expect our technique to be of general value for studying the 3D stereospecificity of dynamic molecular interactions with nanometre resolution.

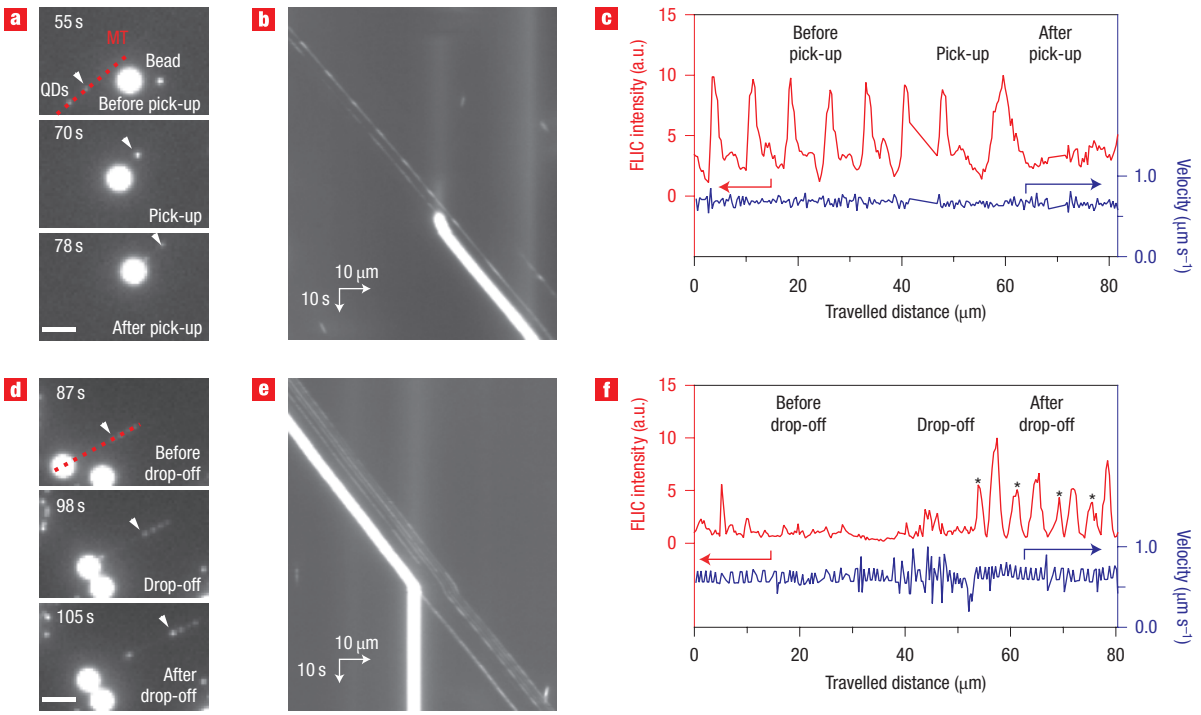

Figure 4 Microtubule rotations during pick-up and drop-off of micrometre-sized cargo. a, Fluorescent images of a motile microtubule (MT, red dotted line) with two QDs (small dots) picking up a 2.8-μm bead (large dot) at 70 s. **b**, Space–time intensity plot (kymograph) of QDs and the bead along the path of the motile microtubule in **a**. **c**, Intensity (red) and velocity (blue) versus distance travelled for the QD marked with an arrowhead in **a**. The singular broadened peak after initial cargo pick-up is presumably caused by slight slippage of the cargo. **d–f**, Corresponding images of bead drop-off at 98 s. Smaller satellite peaks (asterisks in **f**) were most likely due to an additional nearby QD. Such an occasionally high QD density may be due to the high biotinylation ratios used to ensure that QD labelling coincided with cargos on the same microtubule. The scale bars in **a** and **d** are 5 μm.

METHODS

MOTOR PROTEINS AND MICROTUBULES

We used full-length *Drosophila* kinesin-1 that was purified by applying published protocols[26]. GMP-CPP microtubules were grown for 2 h at 37 °C from a 100-μl BRB80 (80 mM Pipes (Sigma), pH 6.9, with KOH (VWR), 1 mM EGTA (Sigma), 1 mM $MgCl_2$ (VWR)) solution supplemented by 2 μM tubulin (53% unlabelled porcine, 45% Alexa 488-labelled porcine, 2% biotinylated bovine tubulin for Figs 2 and 3 and 45% unlabelled, 10% rhodamine-labelled, 45% biotinylated bovine tubulin for Fig. 4), 1 mM GMP-CPP (Jena Bioscience) and 4 mM $MgCl_2$. BRB80 + Taxol microtubules were grown for 3 h at 37 °C from a 100-μl BRB80 solution supplemented by 2 μM tubulin (53% unlabelled porcine, 45% Alexa 488-labelled porcine, 2% biotinylated bovine tubulin), 0.5 mM Mg-GTP (Roche), 4 mM $MgCl_2$ and 10 μM Taxol (Sigma). Assembled microtubules were centrifuged in a Beckman Airfuge at 100,000*g* for 5 min. The pellet was resuspended in a volume of 200–500 μl BRB80 supplemented by 10 μM taxol. The final tubulin concentrations were 0.4–1.0 μM. All bovine tubulin was purchased from Cytoskeleton. Porcine tubulin was purified from pig brain and partly labelled by Alexa 488 (Invitrogen) as described previously[27].

IN VITRO GLIDING MOTILITY ASSAYS

Microfluidic flow cells were constructed from glass coverslips and silicon wafers using parafilm or double-sided tape as a spacer. Flow cell surfaces were blocked by perfusion of a 0.5 mg ml^{-1} casein (Sigma) solution in BRB80. After 5 min a kinesin-1 solution (100 μg ml^{-1} kinesin-1, 10 μM to 1 mM ATP (Roche), 0.2 mg ml^{-1} casein in BRB80) was allowed to flow into the channel. A further 5 min later the microtubule solution containing 10 μM–1 mM ATP, 10 μM taxol and 0.2 mg ml^{-1} casein in BRB80 was flowed into the channel and microtubules were allowed to bind to the motors for about 5 min. Subsequently, 10 μl of a QD 655 (Invitrogen) containing solution (BRB80, 10 μM to 1 mM ATP, 10 μM taxol, 0.2 mg ml^{-1} casein, 2–50 pM QD 655) flowed in. After 5–10 min of incubation, excess QDs were washed away with 60–100 μl of a motility solution (BRB80, 10 μM to 1 mM ATP, 10 μM taxol, 0.2 mg ml^{-1} casein, and an oxygen scavenger mix of 20 mM D-glucose (Sigma), 0.02 mg ml^{-1} glucose oxidase, 0.008 mg ml^{-1} catalase, and 10 mM DTT or 0.5% BME, all from Sigma). For the cargo pick-up and drop-off experiments Dynabeads M-270 streptavidin (0.03–0.1 pM, Dynal, Invitrogen) in a motility solution with 1 mM ATP were additionally flowed through the channel.

OPTICAL IMAGING

Image acquisition was performed using an inverted fluorescence microscope (Zeiss Axiovert 200M) with a ×63 water immersion 1.2 NA objective (Zeiss) in combination with an Andor Ixon DV 897 (Andor) EMCCD camera. For excitation a Lumen 200 metal arc lamp (Prior Scientific Instruments) was used. Cargo pick-up and drop-off experiments were performed on an upright fluorescence microscope (Zeiss Axioplan 2) using a Plan-Neofluar ×40 oil immersion 1.3 NA objective (Zeiss). For experiments that involved dual-colour imaging, that is, when the fluorescence signals of QDs and microtubules were to be captured simultaneously, the red and green channels were separated using a spectral beamsplitter (W-view A8509, Hamamatsu). The signals of the two colour channels were then recorded on two different halves of the same CCD camera chip. To align the dual-colour images with respect to each other multifluorescent tetraspeck beads (0.2 μm diameter, Mo Bi Tec) were diluted 200-fold in BRB80 and additionally perfused into the flow chambers before the flow sequence of the motility assays. Images were recorded in continuous acquisition mode at rates of up to 10 frames s^{-1}. The following filters (Chroma Technology, unless otherwise stated) were used for imaging: exc 475/42 (Semrock), dc 488LP (Semrock) and em dual-band 527-645 (Semrock) for dual-colour detection. In addition, the W-view beamsplitter was equipped with em 531/40 (Semrock), em 660/40, dc 590dcxr and dc Q590dcspxr components. For single-colour detection, either of the green or red detection paths of the W-view beamsplitter was used, and the dichromatic mirrors were replaced by a silver mirror. For cargo pick-up experiments no W-view beamsplitter was installed and a single-band emission filter em 660/40 was used instead.

IMAGE PROCESSING

Single particle tracking was performed using in-house software based on MatLab (Mathworks, Natick, MA). The applied algorithm used 2D Gaussian fitting (least-squares method; variable width of Gaussian) of the pixelated intensity profiles arising from single particles. Plotted FLIC intensity values were derived by integration over the fitted Gaussians. Microtubule tracking was performed by segmenting the filament images and subsequent fitting by various Gaussian-based model functions. Rotational periodicities for the histograms were derived from manual, computer-aided measurements applied to the traces of FLIC intensity versus distance travelled. The sideways deviation was calculated as the orthogonal distance between the QD positions and the centreline of the tracked microtubules.

Received 4 March 2008; accepted 1 July 2008; published 10 August 2008.

References

1. Hess, H., Bachand, G. D. & Vogel, V. Powering nanodevices with biomolecular motors. *Chem. Eur. J.* **10,** 2110–2116 (2004).
2. van den Heuvel, M. G. & Dekker, C. Motor proteins at work for nanotechnology. *Science* **317,** 333–336 (2007).
3. Ray, S., Meyhofer, E., Milligan, R. A. & Howard, J. Kinesin follows the microtubule's protofilament axis. *J. Cell Biol.* **121,** 1083–1093 (1993).
4. Yajima, J. & Cross, R. A. A torque component in the kinesin-1 power stroke. *Nature Chem. Biol.* **1,** 338–341 (2005).
5. Gelles, J., Schnapp, B. J. & Sheetz, M. P. Tracking kinesin-driven movements with nanometre-scale precision. *Nature* **331,** 450–453 (1988).
6. Svoboda, K., Schmidt, C. F., Schnapp, B. J. & Block, S. M. Direct observation of kinesin stepping by optical trapping interferometry. *Nature* **365,** 721–727 (1993).
7. Seitz, A. & Surrey, T. Processive movement of single kinesins on crowded microtubules visualized using quantum dots. *EMBO J.* **25,** 267–277 (2006).
8. Reck-Peterson, S. L. *et al*. Single-molecule analysis of dynein processivity and stepping behaviour. *Cell* **126,** 335–348 (2006).
9. Vale, R. D. *et al*. Direct observation of single kinesin molecules moving along microtubules. *Nature* **380,** 451–453 (1996).
10. Yildiz, A., Tomishige, M., Vale, R. D. & Selvin, P. R. Kinesin walks hand-over-hand. *Science* **303,** 676–678 (2004).
11. Brunner, C., Wahnes, C. & Vogel, V. Cargo pick-up from engineered loading stations by kinesin driven molecular shuttles. *Lab. Chip* **7,** 1263–1271 (2007).
12. Ramachandran, S., Ernst, K. H., Bachand, G. D., Vogel, V. & Hess, H. Selective loading of kinesin-powered molecular shuttles with protein cargo and its application to biosensing. *Small* **2,** 330–334 (2006).
13. Block, S. M., Asbury, C. L., Shaevitz, J. W. & Lang, M. J. Probing the kinesin reaction cycle with a 2D optical force clamp. *Proc. Natl Acad. Sci. USA* **100,** 2351–2356 (2003).
14. Chan, W. C. *et al.* Luminescent quantum dots for multiplexed biological detection and imaging. *Curr. Opin. Biotechnol.* **13,** 40–46 (2002).
15. Mansson, A. *et al.* In vitro sliding of actin filaments labelled with single quantum dots. *Biochem. Biophys. Res. Commun.* **314,** 529–534 (2004).
16. Bachand, G. D. *et al.* Assembly and transport of nanocrystal CdSe quantum dot nanocomposites using microtubules and kinesin motor proteins. *Nano Lett.* **4,** 817–821 (2004).
17. Thompson, R. E., Larson, D. R. & Webb, W. W. Precise nanometre localization analysis for individual fluorescent probes. *Biophys. J.* **82,** 2775–2783 (2002).
18. Lambacher, A. & Fromherz, P. Fluorescence interference-contrast microscopy on oxidized silicon using a monomolecular dye layer. *Appl. Phys. A* **63,** 207–216 (1996).
19. Kerssemakers, J., Howard, J., Hess, H. & Diez, S. The distance that kinesin-1 holds its cargo from the microtubule surface measured by fluorescence interference contrast microscopy. *Proc. Natl Acad. Sci. USA* **103,** 15812–15817 (2006).
20. Nishizaka, T., Yagi, T., Tanaka, Y. & Ishiwata, S. Right-handed rotation of an actin filament in an in vitro motile system. *Nature* **361,** 269–271 (1993).
21. Mimori, Y. & Mikinoumura, T. Extrusion of rotating microtubules on the dynein-track from a microtubule–dynein gamma-complex. *Cell Motil. Cytoskeleton* **30,** 17–25 (1995).
22. Vale, R. D. & Toyoshima, Y. Y. Rotation and translocation of microtubules *in vitro* induced by dyneins from *Tetrahymena* cilia. *Cell* **52,** 459–469 (1988).
23. Walker, R. A., Salmon, E. D. & Endow, S. A. The *Drosophila* claret segregation protein is a minus-end directed motor molecule. *Nature* **347,** 780–782 (1990).
24. Hyman, A. A., Chretien, D., Arnal, I. & Wade, R. H. Structural changes accompanying GTP hydrolysis in microtubules: information from a slowly hydrolyzable analogue guanylyl-(alpha, beta)-methylene-diphosphonate. *J. Cell Biol.* **128,** 117–125 (1995).
25. Wang, Z. & Sheetz, M. P. The C-terminus of tubulin increases cytoplasmic dynein and kinesin processivity. *Biophys. J.* **78,** 1955–1964 (2000).
26. Hancock, W. O. & Howard, J. Processivity of the motor protein kinesin requires two heads. *J. Cell Biol.* **140,** 1395–1405 (1998).
27. Hunter, A. W. *et al*. The kinesin-related protein MCAK is a microtubule depolymerase that forms an ATP-hydrolyzing complex at microtubule ends. *Mol. Cell* **11,** 445–457 (2003).
28. Andreu, J. M. *et al.* Low resolution structure of microtubules in solution. Synchrotron X-ray scattering and electron microscopy of taxol-induced microtubules assembled from purified tubulin in comparison with glycerol and MAP-induced microtubules. *J. Mol. Biol.* **226,** 169–184 (1992).
29. Wade, R. H. & Chretien, D. Cryoelectron microscopy of microtubules. *J. Struct. Biol.* **110,** 1–27 (1993).

Supplementary Information accompanies this paper at www.nature.com/naturenanotechnology.

Acknowledgements

The authors thank C. Bräuer, D. Naumburger and F. Friedrich for technical support, D. Zwicker and Y. Kalaidzidis for help with the tracking algorithms, G. Brouhard for advice on the subtilisin digestion of microtubules, C. Leduc, J. Kerssemakers, J. Helenius, S. Mashaghi and J. Howard for fruitful discussions, and C. Gell and T. Korten for comments on the manuscript. This work was supported by the German Federal Ministry of Education and Research (grant 03 N 8712) and the Max-Planck Society.

Author contributions

B.N. and S.D. conceived and designed the experiments. B.N. performed the experiments. F.R. developed the nanometre tracking software. B.N. and F.R. analysed the data. All authors discussed the results. B.N. and S.D. co-wrote the paper.

Author information

Reprints and permission information is available online at http://npg.nature.com/reprintsandpermissions/. Correspondence and requests for materials should be addressed to S.D.